Ultimate sensitivity of superconducting single-photon detectors in the visible to infrared range

A. Verevkin[1], J. Zhang, A. Pearlman, W. Slysz, and Roman Sobolewski
University of Rochester, Rochester, NY 14627-0231, USA
A. Korneev, P. Kouminov, O. Okunev, G. Chulkova, and G. Gol'tsman
Moscow State Pedagogical University, Moscow 119435, Russia

ABSTRACT

We present our quantum efficiency (*QE*) and noise equivalent power (*NEP*) measurements of the meander-type ultrathin NbN superconducting single-photon detector in the visible to infrared radiation range. The nanostructured devices with 3.5-nm film thickness demonstrate *QE* up to ~10% at 1.3 – 1.55 μm wavelength, and up to 20% in the entire visible range. The detectors are sensitive to infrared radiation with the wavelengths down to ~10 μm. *NEP* of about 2×10^{-18} W/Hz$^{1/2}$ was obtained at 1.3 μm wavelength. Such high sensitivity together with GHz-range counting speed, make NbN photon counters very promising for efficient, ultrafast quantum communications and another applications. We discuss the origin of dark counts in our devices and their ultimate sensitivity in terms of the resistive fluctuations in our superconducting nanostructured devices.

INTRODUCTION

Superconducting single-photon detectors (SSPDs) [1] based on ultrathin, submicron-width NbN superconducting meander lines have already found several practical applications [2-4], based on their picosecond-range response time, low jitter, and low dark counts. The SSPD ability to efficiently count single photons has been explained within a phenomenological hot-electron photoresponse model [1, 5]. This model describes formation and subsequent growth of a resistive hotspot in a very narrow, current-biased superconducting stripe upon the single-photon absorption event [6], [7]. The hotspot formation is followed by supercurrent redistribution, leading to a transient voltage response signal [8]. The NbN-based SSPDs are able to efficiently detect single photons in the wavelength range from ultra-violet to near infrared (IR) [4], [9] at a GHz-range counting speed [10]. They work at the 4-K temperature level, which allows a long-term, no-interruption work, when using modern closed-cycle refrigerators. Their fiber-optical coupling makes easy to perform room temperature photon-counting experiments.

The aim of this presentation is to demonstrate the performance of our new SSPDs, fabricated from 3.5-nm-thick NbN films. We found a significant (up to two orders of magnitude) increase of quantum efficiency (*QE*) in such detectors, as compared with the 10-nm-thick structures [4]. Our new 3.5-nm devices exhibit *QE* up to ~10% at near IR and above 15% in the visible range. We associate such an improvement of *QE* with the large increase of a hotspot size in thinner NbN films. We also present here the sensitivity performance of our detectors. Knowing the dark counting rate and its bias current dependence we were able to determine a noise equivalent power *(NEP)*, which is widely regarded to be the best measure of the detector sensitivity. For our best devices the *NEP* reaches 2×10^{-18} W/Hz$^{1/2}$ at 1.3 μm wavelength.

EXPERIMENTAL DETAILS

The devices used in our experiments were 10×10-μm^2-area size NbN superconducting meander-type structures with the film thickness d = 3.5 nm, the nominal stripe width w ~ 200 nm, and the gap between the meander stripes of about 300 nm (filling factor ~0.4). The details of our fabrication process are

Contact information for A. Verevkin- Email: verevkin@ece.rochester.edu

described in [11]. Critical current density of devices varied within 5-8 MA/cm^2 range at 4.2 K and superconducting transition temperature T_c was about 10 K.

The devices under study were wire-bonded to a 50-Ω microwave stripe line and mounted on a cold base plate maintained at 4.2 K in vacuum inside either a liquid-helium dewar or a two-stage cryocooler. Voltage pulses generated by the SSPD under illumination were amplified by 1-2 GHz bandwidth, room-temperature amplifier and fed to a photon counter. Radiation from different laser sources was delivered inside the cryostat through free space, or using a standard multimode 50-μm-core-diameter fiber, and focused by collimator on the device plane inside the cryostat. In *NEP* measurements the incoming 1.3-μm radiation from a luminescence diode was filtered inside cryostat with a cold (4.2 K) 0.9-1.6 μm bandpass filter to block long-wavelength thermal background as well as any parasitic visible light.

EXPERIMENTAL RESULTS

Our latest 3.5-nm-thick devices demonstrate significantly larger *QE*, as compared to the previous, 10-nm-thick devices [3]. The improvement is about two orders of magnitude in the visible range, and even larger for IR photons. Figure 1 presents *QE* versus wavelength for a 10 × 10-μm^2 area, 3.5-nm-thick NbN SSPD. We believe that in the visible range our latest SSPDs have already reached the limiting intrinsic *QE*, corresponding to counting of all photons incident upon the device's superconducting stripe. As the result, *QE* tends to be independent of radiation wavelength in the visible range. In addition, the entire spectral dependence shown in Fig. 1 is significantly flatter than the dependence characteristic for the 10-nm-thick devices [4]. The reason for such a significant improvement of *QE* in the thinner SSPDs is quite obvious – the normal resistance hotspot area in those devices is significantly larger, as it should be roughly inversely proportional to the film thickness [6].

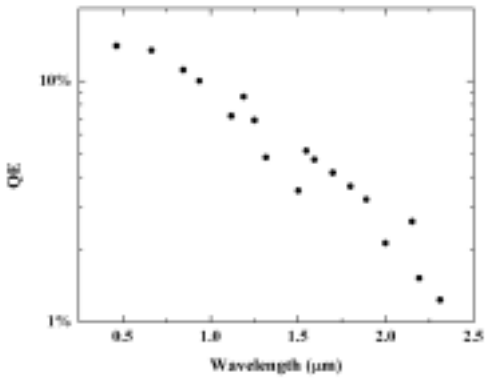

Fig. 1. Spectral dependence of *QE* for a typical 10x10-μm^2 area, 3.5-nm-thick NbN meander detector. Temperature is 4.2 K with the current bias is equal to $0.9I_c$.

The other parameter, besides *QE*, responsible for ultimate sensitivity of single-photon detectors is the dark counting rate *R*. *R*, together with *QE*, determines the *NEP* of single-photon detectors in the following manner:

$$NEP = \frac{h\upsilon}{QE}\sqrt{2R}\ . \qquad (1)$$

The *R(I)* dependence, shown in Fig 2 (right vertical axis), demonstrates the activation law $R = a\times\exp(b\times I/I_c)$ in the whole biasing range used in our experiments ($0.98 > I/I_c > 0.85$), where *a* and *b* are constants, and I_c is the detector critical current. The activation-type behavior of *R(I)* can be observed within five orders of magnitudes range and is independent of the device size or the actual superconductor stripe width. Left vertical axis in Fig. 2 corresponds to *QE* dependence on the normalized current bias. As in the case of *R*, we observe an exponential decrease of *QE* with the I/I_c ratio decrease, but at least for bias currents close to I_c, the *QE* drop is relatively slow.

Figure 3 presents *NEP* versus I/I_c, obtained using Eq. (1) and the experimental results on both *QE* and *R* shown in Fig. 2 within the $0.98 > I/I_c > 0.85$ range (closed dots). We note that *NEP* of about 2×10^{-18}

W/Hz$^{1/2}$ has been achieved for $I/I_c = 0.87$. This is the best sensitivity in the near-IR range, ever reported for a single-photon detector operating at 4 K temperature level. As we can see in Fig. 3, the *NEP* rapidly decreases with the bias decrease, since close to I_c, R is a much stronger function of I/I_c then *QE*. Extrapolating the R data from Fig. 2 and extending the *NEP* plot into low bias using experimental *QE* points from Fig. 2, we can reach *NEP* below 10^{-20} W/Hz$^{1/2}$.

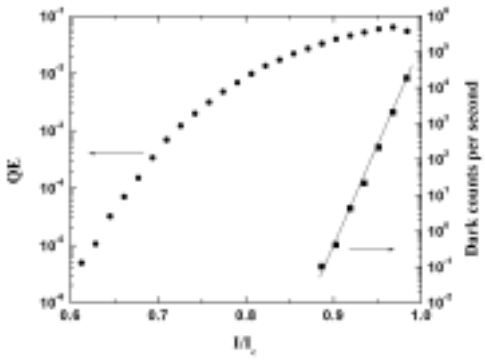

Fig. 2. *QE* and dark counting rate R versus the normalized bias current, measured for a 3.5-nm-thick, 10x10-μm^2 area SSPD at 1.3-μm wavelength. Solid line illustrates the activation-type law of the R dependence on the detector bias.

For low I/I_c values, the *NEP* saturates, due to the very fast drop of the *QE* curve at low current bias (Fig. 2). The physical meaning of this saturation phenomenon is quite simple – the detector becomes insensitive to incident radiation and the *QE* slope follows the R slope, as the supercurrent redistribution is too small to produce a voltage response at such low biases.

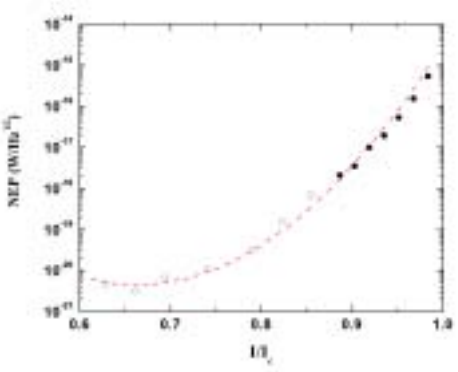

Fig. 3. *NEP* versus the normalized bias for a 3.5-nm-thick, 10x10-μm^2 area SSPD at 1.3-μm wavelength. Closed circles correspond to experimental data presented in Fig. 2, while open circles represent the extrapolated result based on the measured *QE* and the R (see Fig. 2) interpolated to the low bias currents. Dashed line is a guide to the eye.

DISCUSSION

Dark counts and their rate R play the basic role for the ultimate sensitivity of any single-photon detector, as we can see from Eq. (1). The origin of dark counts in our NbN SSPDs in absence of any incident photon flux or significant thermal background fluctuations represents an interesting physical problem. We believe that the observed dark counts are mainly due to resistive (or, equivalently, superconducting) fluctuations in our NbN superconducting stripes. Such fluctuations were observed in one-dimensional (1-D) superconducting stripes at low temperatures and have been discussed in terms of quantum phase slip centers (PSCs) [12-14]. We have already pointed out to the role of such fluctuations in the context of the experimentally measured, exponential spectral dependence of *QE* [4].

The 1-D picture is not fully adequate for our devices. The thickness d of the NbN superconducting stripe is indeed close to the BCS coherence length ξ, but the stripe width w is significantly larger than ξ. On the other hand, the 1-D approach seems to be productive to improve our understanding of the problem and

for development of a quantitative model of dark counts in our NbN SSPDs. A significant extension of the 1-D phase slips formation process [15] towards the case of wider stripes ($w >> \xi$) was obtained at low temperatures at the presence of bias currents close to I_c [16,17]. It was shown in [16] that the essential features of the PSC model are preserved, when compared with the 1-D case, including the quasiparticle diffusion length, and the drop of the pair chemical potential over the ξ distance. A general, theoretical investigation of the problem in the 2-D case was proposed in [18], and it was recently used to study of PSC formation in Nb and YBCO bridges [19]. The main conclusion made in [19] was that the PSCs could occur in superconducting stripes more frequently than it is generally admitted by modern theories for uniform clean superconductors at temperatures well below T_c. Authors in [19] suggested that this latter observation could support the idea proposed in [18], namely that the PSCs are formed from microscopic normal-state hotspots existing in granular films.

We strongly believe that the above case applies to our NbN films. Detailed, atomic-force microscope and electron microscope studies did not show any evidence of nm-scale defects in our NbN films. However, our structures are characterized by a negative resistivity temperature coefficient within the 20-300 K temperature range, what is often associated with the existence of granular microstructure in thin NbN films [20]. Consequently, in agreement with the concept proposed in [18],[19], the origin dark counts in our structures is very likely to be associated with granularity of our NbN films. More detailed study on this subject will be presented elsewhere.

This work was funded by the US Air Force Office for Scientific Research grant F49620-01-1-0463 (Rochester) and by the RFBR grant 02-02-16774 (Moscow). Additional support was provided by the NPTest, San Jose, CA.

REFERENCES

1. G. N. Gol'tsman, O. Okunev, G. Chulkova, A. Lipatov, A. Semenov, K. Smirnov, B. Voronov, A. Dzardanov, C. Williams, and R. Sobolewski, *Appl. Phys. Lett. 79*, 705 (2001).
2. S. Somani, S. Kasapi, K. Wilsher, W. Lo, R. Sobolewski and G. Gol'tsman, *J. Vac. Sci. Technol. B 19*, 2766 (2001).
3. R. Sobolewski, A. Verevkin, G. N. Gol'tsman, A. Lipatov, and K. Wilsher, *IEEE Trans. Appl. Supercon*. (June 2003).
4. A. Verevkin, J. Zhang, R. Sobolewski, G. Chulkova, A. Korneev, A. Lipatov, O. Okunev, A. Semenov, and G. N. Gol'tsman, *Appl. Phys. Lett. 80*, 4687 (2002).
5. A. D. Semenov, G. N. Gol'tsman, and A. A. Korneev, *Physica C 351*, 349 (2001).
6. A. M. Kadin and M. W. Johnson, *Appl. Phys. Lett. 69*, 3938 (1996).
7. K.S. Il'in, I. I. Milostnaya, A. A. Verevkin, G. N. Gol'tsman, E. M. Gershenzon, and R. Sobolewski, *Appl. Phys. Lett. 73*, 3938 (1998).
8. J. Zhang, W. Slysz, A. Verevkin, R. Sobolewski, O. Okunev, and G. N. Gol'tsman, *Phys. Rev. B 67*, 132508 (2003).
9. A. Lipatov, O. Okunev, K. Smirnov, G. Chulkova, A. Korneev, P. Kouminov, G. Gol'tsman, J. Zhang, W. Slysz, A. Verevkin, and R. Sobolewski, *Supercon. Sci. and Tech.* 15, 1689 (2002).
10. J. Zhang, W. Slysz, A. Verevkin, O. Okunev, G. Chulkova, A. Korneev, A. Lipatov, G. N. Gol'tsman, and R. Sobolewski, *IEEE Trans. Appl. Supercon*. (June 2003).
11. G. N. Gol'tsman, K. Smirnov, P. Kouminov, B. Voronov, N. Kaurova, V. Drakinsky J. Zhang, A. Verevkin, and R. Sobolewski, *IEEE Trans. Appl. Supercon*. (June 2003).
12. C. N. Lau, N. Markovic, M. Bockrath, A. Bezryadin, and M. Tinkham, *Phys. Rev. Lett. 87*, 217003 (2001).
13. M. Tinkham and C.N. Lau, *Appl.Phys. Lett 80*, 2946 (2002).
14. A. Bezryadin, C. N. Lau, and M. Tinkham, *Nature 404*, 971 (2000).
15. W.J. Skocpol, M.R. Beasley, and M. Tinkham, *J. Low Temp. Phys. 16*, 145 (1974).
16. V.G. Volotskaya, I.M. Dmitrenko, L.E. Musienko, and A.G. Sivakov, *Sov. J. Low Temp. Phys. 7*, 188 (1981); *Sov. J. Low Temp. Phys. 10*, 179 (1984).
17. A. Garzarella and C.J. Martoff, *J. Appl. Phys. 79*, 2426 (1996).
18. A. Weber and L. Kramer, *J. Low. Temp. Phys. 84*, 289 (1991).
19. J.-P. Maneval, F. Boyer, K. Harrabi, and F.-R. Ladan, *J. of Superconductivity 14*, 347 (2001).
20. J.-H. Tyan, and J.T. Lue, *Journal of Appl. Physics 75*, 325 (1994).